Journal Pre-proofs

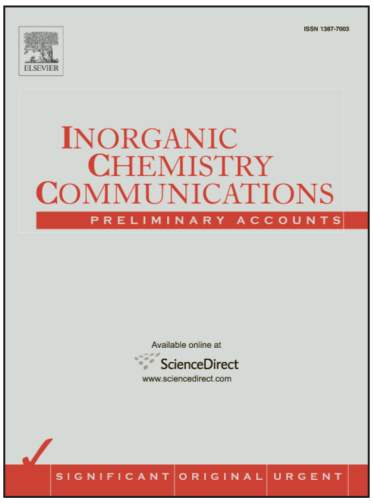

Short communication

Oxadiazole based Os(IV) compounds as potential DNA intercalator and cytotoxic agents

Bharat H. Pursuwani, Bhupesh S. Bhatt, Foram U. Vaidya, Chandramani Pathak, Mohan N. Patel

PII: S1387-7003(20)30660-2
DOI: https://doi.org/10.1016/j.inoche.2020.108070
Reference: INOCHE 108070

To appear in: *Inorganic Chemistry Communications*

Received Date: 27 April 2020
Revised Date: 25 June 2020
Accepted Date: 28 June 2020

Please cite this article as: B.H. Pursuwani, B.S. Bhatt, F.U. Vaidya, C. Pathak, M.N. Patel, Oxadiazole based Os(IV) compounds as potential DNA intercalator and cytotoxic agents, *Inorganic Chemistry Communications* (2020), doi: https://doi.org/10.1016/j.inoche.2020.108070

Oxadiazole based Os(IV) compounds as potential DNA intercalator and cytotoxic agents

Bharat H. Pursuwani, Bhupesh S. Bhatt, Foram U. Vaidya, Chandramani Pathak and Mohan N. Patel*

Department of Chemistry, Sardar Patel University,
Vallabh Vidyanagar–388 120, Gujarat, India.
Corresponding author. Tel.: +91 2692 226856
E-mail: jeenen@gmail.com

Abstract

Os(IV) compounds and ligands have been synthesized and well characterized. DNA cleavage tendency of compounds has been evaluated using gel electrophoresis and binding behavior has been evaluated by viscosity measurements, absorption titration, fluorescence, and docking studies. All the compounds show the intercalation mode of binding. The binding constant of complexes falls at about 1.8-7.6×10^4 M^{-1}. Bacteriostatic activity of compounds has been evaluated on a series of gram^{+ve} and gram^{-ve} bacteria in terms of their MIC values. Also, the compounds have been screened for *in vivo* and *in vitro* cytotoxicity assays on *S. Pombe* cell's DNA and HCT-116 cell line. LC_{50} of ligands and Os(IV) complexes are in the range of 7.92-19.91 and 4.00- 11.74 μg/mL respectively.

Keywords: Os(IV), DNA cleavage, Bacteriostatic, *S.Pombe*, HCT-116.

1. Introduction

Nitrogen and oxygen atoms bearing fused heterocycles have been proved successful in keeping footprint in the world of medicinal chemistry [1-3]. Oxadiazoles have been proved as successful in bringing a variety of novel drugs.[4] Iso-oxazoles have been explored widely in medicinal chemistry [5, 6]. Iso-oxazoles have been widely used in marketed products such as leflunomide [7], sulfafurazole [8], isooxaflutole, [9] and hymexazol [10] (Supplementary material 1). Oxadiazoles are analogues heterocycles of iso-oxazoles, oxadiazoles moieties fused with phenyl ring exhibit a wide variety of biological activities [11-13]. They have an impactful biological role, efficacy, and pharmacokinetics importance [14]. Various drugs with this parent

moiety have been proved successful, such as sulfamethoxazole, which has been proved as antibiotic and proved to have a wide broad spectrum against bacteria [15]. Risperidone has been effective in the treatment of schizophrenia[16]. These have been a class of highly stable electron donating species. Synthesis of oxadiazoles has been widely explored in synthetic organic chemistry [17]. 1,3,4-Oxadiazoles have been proved as effective tuberculosis analogues [18]. Oxadiazole has been a similar class of compounds. Geometry and conformational environment of molecules are important to adhere interaction mechanism of the molecule with DNA [19, 20]. Synthesis and biological applications of oxadiazole heterocycles have been widely explored [21, 22]. Oxadiazole nucleus based ruthenium(II) complexes have been synthesized and reported in the literature [23]. Oxadiazole heterocycles have also proved to be anticonvulsant and antidepressant agents [24]. These class of heterocyclic ligands readily coordinate with 5d transition metal ions [25]. Metal complexes have been popular amongst inorganic chemists to explore a wide plethora of aspects in biological applications [26, 27]**.** Osmium metal ion based complexes are quite inert in comparison to ruthenium which provides stability to molecule [28]. Osmium metal ion based complexes have been proved successful in resisting the growth of tumor cells, which highlights its potentiality in its anti-cancer behavior [29, 30]. They have been also proved successful in photo-cleavage of macromolecules [31]. Osmium complexes with tetrazolo quinoline moiety have been reported to have good biological efficacy and DNA interaction mode [29]. Osmium compounds have been most investigated as non-platinum metallodrug undergoing clinical screenings [28]. These have proved to have more selectivity towards diseased cells [32]. FY026 has been proved to be a successful osmium class of drug over HCT-116 cell line and has greater tolerability compared to ruthenium class of drugs which are of pharmacokinetic importance [33]. Osmium complex with azopyridine nucleus has been proved to be effective at sub-micromolar concentration over wide variety of cell lines and are competing to ruthenium complexes and cis-platin analogues [34].

2. Experimental

General method for synthesis of ligands, metal salt, and complexes

Ligand L^1 i.e. 1-(2-(4-chlorophenyl)-5-phenyl-1,3,4-oxadiazol-3(2H)-yl)ethan-1-one have been synthesized by reacting 4-chloro benzaldehyde (2 g, 14 mmol) with (1.93 g, 14 mmol) benzhydrazide to form Schiff base in presence of potassium hydroxide (0.39 g, 7 mmol). The Schiff base formed (1 g, 3 mmol) has been further refluxed with acetic anhydride (0.36 mL, 3

mmol) to form ligand L^1. $(NH_4)_2OsBr_6$ has been synthesized by refluxing OsO_4 (25 mg dissolved in 25 mL millipore water) with hydrobromic acid (9 mL) at 80 °C for the period of 2h. The resulting solution has been mixed with ammonium bromide (0.36 g) at room temperature with constant stirring. The solution has been kept in a deep freezer at 2-4 °C till the salt formation [35, 36]. Complex C^1 i.e. tetrabromido(1-(2-(4-chlorophenyl)-5-phenyl-1,3,4-oxadiazol-3(2H)-yl)ethan-1-one)osmium(IV) has been synthesized using $(NH_4)_2OsBr_6$ (60 mg, 8 mmol) and ligand L^1 (25 mg, 8 mmol).

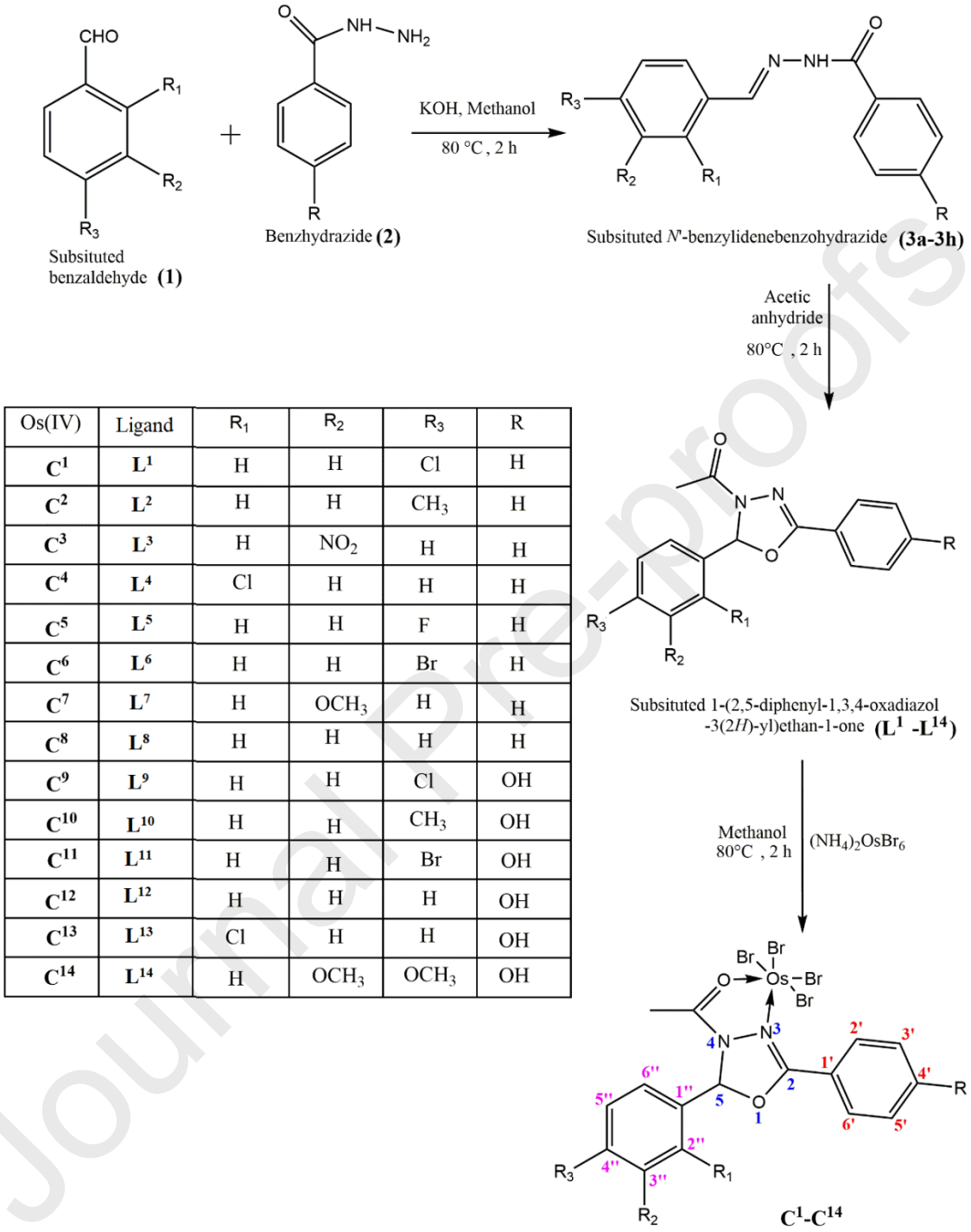

Os(IV)	Ligand	R_1	R_2	R_3	R
C^1	**L^1**	H	H	Cl	H
C^2	**L^2**	H	H	CH_3	H
C^3	**L^3**	H	NO_2	H	H
C^4	**L^4**	Cl	H	H	H
C^5	**L^5**	H	H	F	H
C^6	**L^6**	H	H	Br	H
C^7	**L^7**	H	OCH_3	H	H
C^8	**L^8**	H	H	H	H
C^9	**L^9**	H	H	Cl	OH
C^{10}	**L^{10}**	H	H	CH_3	OH
C^{11}	**L^{11}**	H	H	Br	OH
C^{12}	**L^{12}**	H	H	H	OH
C^{13}	**L^{13}**	Cl	H	H	OH
C^{14}	**L^{14}**	H	OCH_3	OCH_3	OH

Scheme 1. Synthesis of compounds.

3. Results and discussion

3.1. Characterization

Ligands L^1-L^8 have been synthesized by benzhydrazide as reactant. In ^{1}H-NMR, aromatic proton region of ligand L^1 falls in the range of 7.30-8.48 δ ppm. Aliphatic methine proton is justified at a signal of 6.789 δ ppm. Methyl protons show its presence at 2.59 δ ppm. Ligands L^9-L^{14} have been synthesized by 4-hydroxy benzhydrazide as reactant. In ligand L^9, aromatic proton region is justified at 7.51-7.94 δ ppm. Aliphatic methine proton shows its presence at 6.77 δ ppm. Methyl protons and hydroxy proton show its presence at 1.97 and 12.03 δ ppm respectively. In ligand L^1, there are 5 quaternary carbon signals observed. Carbonyl carbon falls at 163.2 δ ppm. Whereas carbons labeled C2, C1', C1'' and C4'' show its presence at 145.9, 135.2, 134.7, and 124.1 respectively. Aromatic methine carbons are well justified at 133.9, 130.1, 129.3, 129.0 and 123.5 assigned to (C2', C3'), C4', (C5', C6'), (C2'', C3'') and (C5'', C6'') respectively. Aliphatic carbon C5 shows its presence at 83.53 δ ppm whereas, methyl functionality as primary carbon signal falls at 25.15 δ ppm. In ligand L^9, there are 6 quaternary carbon signals observed. Carbonyl carbon falls at 163.7 δ ppm. Whereas carbons labeled C2, C1', C4', C1'' and C4'' show its presence at 146.8, 137.4, 137.3, 132.3 and 131.3 respectively. Aromatic methine carbons are well justified at 133.7, 131.4, 128.9 and 128.1 assigned to (C2', C3'), (C5', C6'), (C2'', C3'') and (C5'', C6'') respectively. Aliphatic carbon C5 shows its presence at 83.22 δ ppm whereas, methyl functionality as primary carbon signal falls at 25.40 δ ppm. A detailed experimental section has been given in supplementary material 2. ^{1}H-NMR and ^{13}C-APT spectra of all the ligands is given in supplementary materials 3 and 4. ICP-OES data justifies metal percentage present in complexes relative to their theoretical values.

LC-MS spectrum of ligand L^1 shows a high intense base peak at 258 m/z whereas mass peak is obtained at 300 m/z. Complex C^1 has been characterized using ESI-MS spectrometry. Molecular ion peak of complex is observed at 810.59 m/z with [M+], [M+2], [M+4], [M+6] and [M+8] peaks. In ligand L^1, the conjugated methine group shows its presence at 3032 cm^{-1}, which shifts slightly to high frequency 3044 cm^{-1} in case of its respective Os(IV) complex C^1. The presence of C-N, C-H, C=C, and C=O bonds in ligands and complexes are justified at 1551, 1366, 1651 and 1605 cm^{-1} to 3044, 1560, 1370, 1655, and 1610 cm^{-1} respectively. Further, N-Os bond is justified at 486 cm^{-1} which move towards higher frequency in N-Os-Br bond at 671 cm^{-1} due to

electron withdrawing behavior of inductive bromine. In complex C^9, bands are relatively shifted compare to ligand L^9. The ν(=C-H), ν(C-N), ν(C-H), ν(C=C), ν(C=O) bands are observed at 3083, 1589, 1402, 1652, 1625 cm^{-1}, respectively. Additionally, ν(N-Os) band is observed at 447 cm^{-1}, whereas ν(N-Os-Br) linkage is justified its presence at 671 cm^{-1}. LC-MS spectra of ligands and ESI-MS spectrum with fragmentation pattern of the complex are given in supplementary materials 5 and 6. IR spectra and CHNS elemental analysis data are given in supplementary materials 7 and 8 respectively.

Magnetic property exhibited by Os(IV) complexes has been measured using Guoy's balance. All the Osmium(IV) complexes bear 2.70-2.80 B.M. with low spin electronic configuration t_{2g}^4 e_g^0 proving paramagnetic behavior containing d^2sp^3 hybridization and possess octahedral geometry [37]. Conductance measurements have been carried out using DMSO solubilized test compounds which shows non-electrolytic behavior. The electronic spectral study concludes that ligands show the transition in the range of 222-284 nm, whereas their respective Os(IV) complexes show bands in the range of 222-296 nm. In complex C^1, bands at 284, 340, and 458 nm are assigned to n-π*, π-π*, and d-d transitions, respectively. This adds support to electronic spectral study in justifying octahedral behavior and paramagnetic behavior exhibited by the Os(IV) compounds.

3.2. Biological activities

3.2.1. DNA binding and cleavage activity

Compounds have interacted in the presence and absence of HS-DNA solution taking the ethidium bromide as reference. Flow time taken by Os(IV) complexes has been relatively higher compared to their respective ligands. Plots in figure 1 show an increase in viscosity of compounds with an increase in concentration of compounds. Comparing ligands amongst series, it can be concluded that ligands L^9-L^{14} took more flow time compared to ligands L^1-L^8 due to the presence of electron releasing hydroxy functionality which enhances interaction and π character of the ring while interacting with HS-DNA solution in thermostatic viscometry bath. All the ligands and Os(IV) complexes show partial intercalation mode of binding [38].

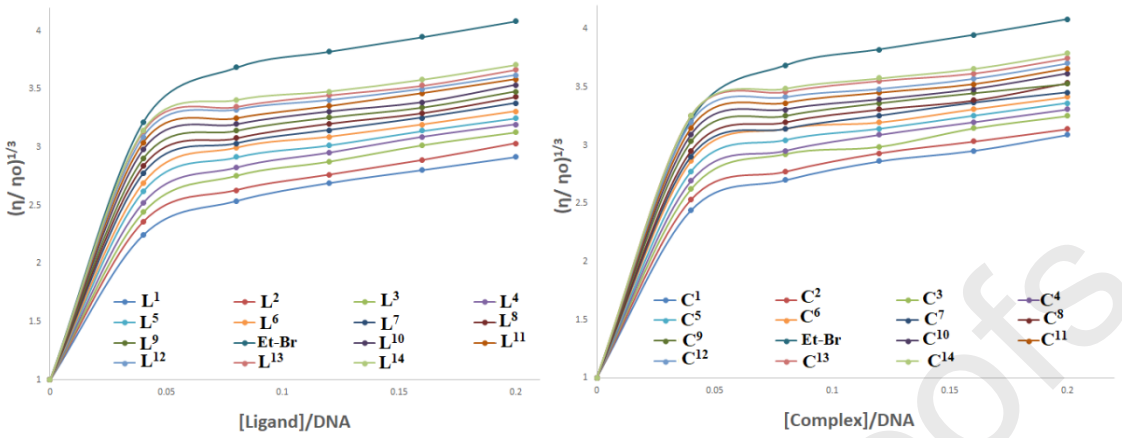

Fig. 1. The plot of effect on relative viscosity of HS- DNA under the influence of an increasing amount of L^1-L^{14} and complexes C^1-C^{14} at 27±0.1 °C in phosphate buffer (pH 7.2)

Os(IV) complexes and ligands have been interacted with B-DNA receptor to evaluate minimum energy acquired by molecules in the best possible flexible conformational structure allowed to run in docking processing software Hex 6.0. Docked images of the interaction of all the compounds are presented in supplementary material 9. There has been an π-π stacking interactions observed between compound and phosphate backbone when compounds interacted with $d(CGCCGAATTCGCCG)_2$ sequence. Compounds intercalate between A-T rich region of DNA. This adds additional proof to titrimetric data and viscometric measurement in showing effective binding by compounds while interacted with DNA. Docking energy of ligands and Os(IV) complexes are given in supplementary material 10.

Upon absorption titrimetric analysis in the absence and varying concentration of DNA solution, a decrease in absorbance has been observed resulting in a slight hypochromism shift. Comparing Os(IV) complexes and their ligands, it is observed that intrinsic binding constant and relative shift in percentage hypochromism is greater in complexes than their respective ligands because of bonding of metal with four bromine atoms which allow dominating π-π stacking interaction between π character of the ring with the lone pairs of nitrogen atom bases of the macromolecule. The interaction is steady and a relatively small shift in absorbance is observed accounting to justify the intercalation mode of binding. Intrinsic binding constant and percentage hypochromism of compounds have been calculated and are given in supplementary material 11.

Figure 2 shows absorption titration curve of complex C^1. The binding constants of Os(IV) complexes are higher than that of copper(II) complexes [39].

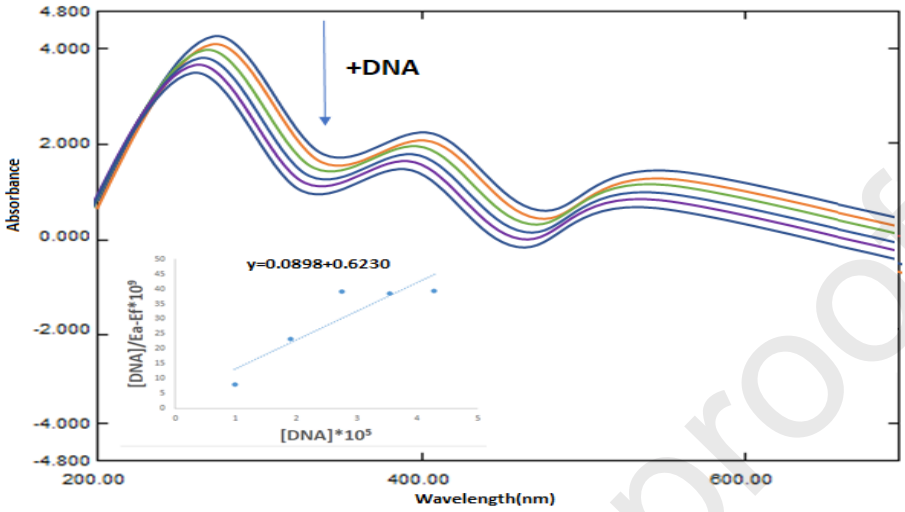

Fig. 2. Absorption spectral changes on addition of HS-DNA to the solution of complex I (after incubating it for 10 min. at room temperature in phosphate buffer. Graph: plot of $[DNA]/(\varepsilon_a-\varepsilon_f)$ vs. [DNA]. (Arrow shows the change in absorption with an increase in the concentration of DNA) amount of complexes and EtBr at 27±0.1 ^oC in phosphate buffer (pH 7.2)

Os(IV) complexes do not show fluorescence at room temperature because of the limitations of quenching ethidium bromide probe in emission spectra. EB-DNA emission band is observed at 470 nm, which is subjected to excitation at 610 nm. Os(IV) complexes displace EB from EB-DNA adduct in various concentration range, thereby decrease in fluorescence intensity have been observed. The constants have been evaluated using Stern Volmer and Scatchard plots graphically with an accurate regression coefficient (r=3.50). The binding constant, quenching constant and binding sites are presented in supplementary material 12. The plots are represented in figure 3. All the complexes show better binding except C^7, C^9, and C^{10} than reported platinum(II) complexes. Amongst, benzhydrazide derived ligands and complexes C^1-C^8, complex C^7 has electron releasing methoxy functionality which lowers the tendency of binding. While amongst 4-hydroxy benzhydrazide derived ligands and complexes C^9-C^{14}, complex C^9 has electron releasing hydroxy and withdrawing chlorine at para positions of reactants counter and nullify such effect as a result only hyperconjugation forces are active in heterocyclic environment. Whereas, complex C^{10} has

electron releasing hydroxy functionality along with the hyperconjugation effect of the methyl group in the ligand environment. Hence, they dominate in showing effective binding strength.

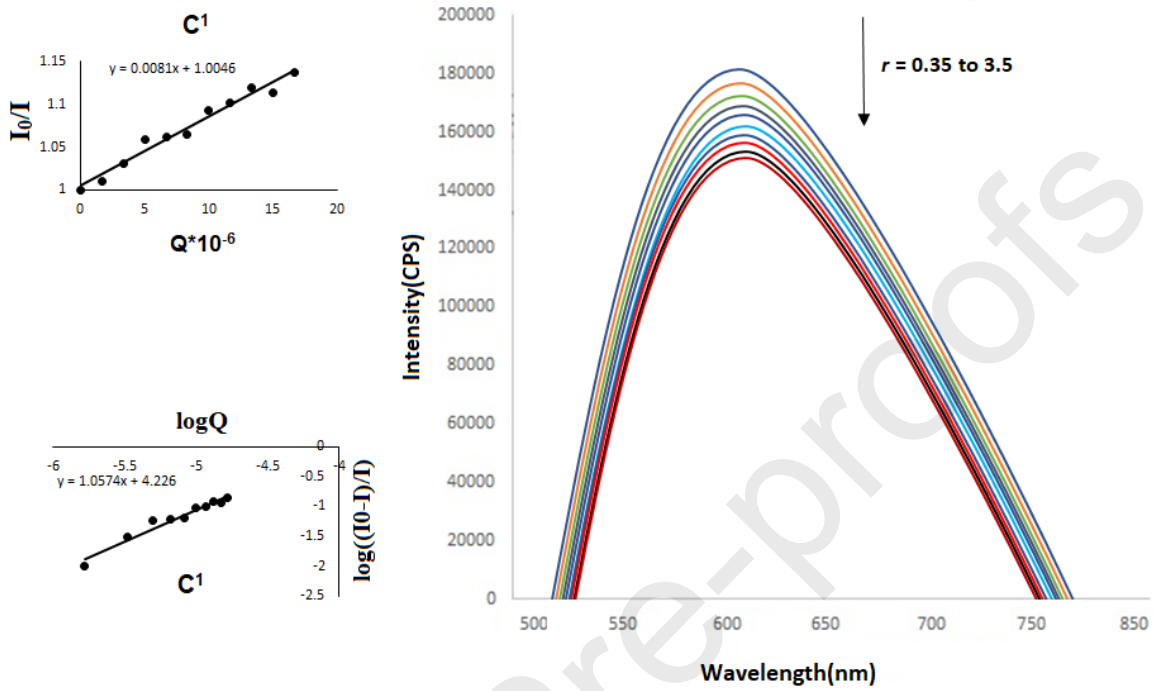

Fig. 3. Fluorescence emission of EB bound to HS-DNA in presence of complex C^1**.** Plots: I0/I vs. [Quencher] and plot of log[I_0-I] vs. log[Q] for the titration of HS-DNA EB system with Os(IV) complex C^1 in 1M phosphate buffer (pH 7.2) medium.

Gel electrophoresis experiment has been carried out on *S. Pombe* cell's DNA. Os(IV) complexes have been proved impactful in degrading DNA when allowed to run over 1% agarose gel in casting apparatus. There have been no smearing observed over untreated DNA samples which conclude the tendency of Os(IV) complexes to show degradation phenomenon of the macromolecule. Relative tendency of complexes to show effective smearing is in order of C^3>C^5>C^4>C^1>C^6>C^8>C^2>C^7>C^{13}>C^9>C^{11}>C^{12}>C^{10}>C^{14}. Complexes C^1-C^8 show better photolytic smearing compare to C^9-C^{14} since the former has electron releasing functionality which pushes the electron cloud of nucleus thereby resisting effective smearing. The presence of nitro functionality readily withdraws electron cloud towards itself ruptures DNA hence there is intense smearing observed in the case of complex C^3. Comparing complexes C^1 and C^4, complex C^4 dominates in showing cleavage property since electron withdrawing chlorine present at ortho position and in former its present at the para position which is closer to nucleus. The same

phenomenon is observed in complexes C^{13} and C^{9}. Photolytic cleavage image photographed by spectrophotometer and intensity visualized by alphadigidoc software is given in figure 4.

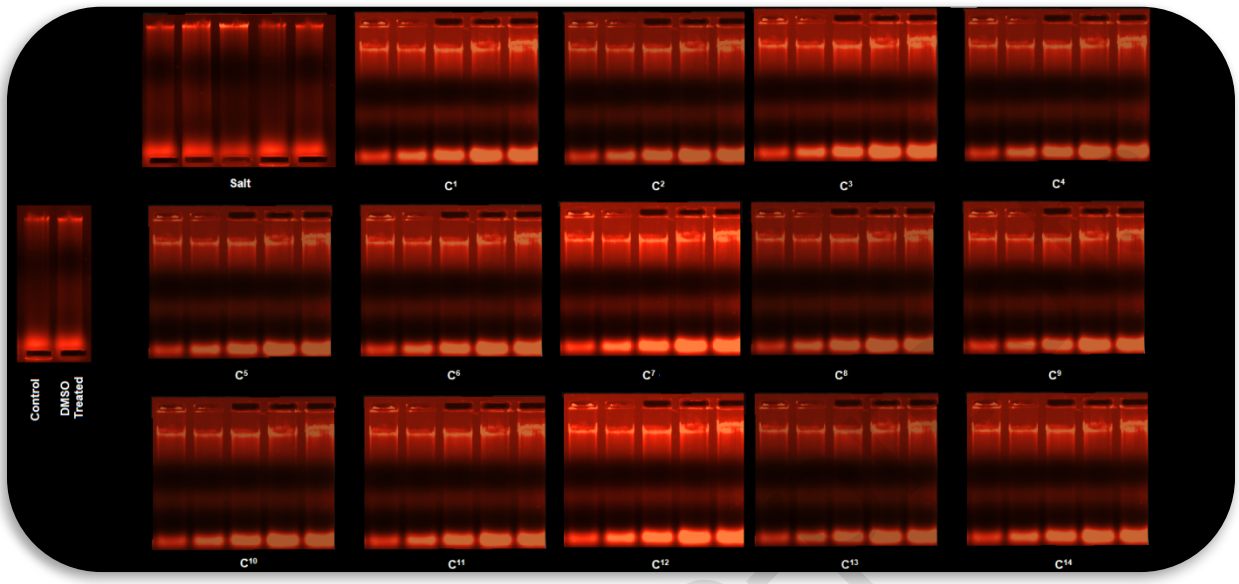

Fig. 4. Photogenic view of cleavage of *S. Pombe* cell's DNA (1 μgL^{-1}) with a series of compounds using 1% agarose gel containing 0.5 (μgL^{-1}) EtBr.

3.1.2. Bacteriostatic activity

Lipids in bacteria play a key role in developing growth and providing an immune response to its walls. Therefore, moieties with functionalities that resist lipid growth or suppress response are equally important to resist the growth of bacteria. Comparing series of ligands, ligands L^{1}-L^{8} show better MIC compare to ligands L^{9}-L^{14} because ligands L^{9}-L^{14} have hydroxy functionality which pushes electron towards the nucleus thereby having less impact on resisting cell wall synthesis of bacteria. On the other hand, ligands L^{1}-L^{8}, there is hyperconjugation of bonds taking part in the absence of any electron withdrawing or releasing functionality which is comparatively more impactful in resisting bacterial growth. Os(IV) complexes have high electron withdrawing bromine atoms able to rupture cell walls of bacteria in resisting the growth of bacteria hence show superior MIC compared to their respective ligands as shown in figure 5. in terms of µM concentration. Ligands and Os(IV) complexes show MIC in range of 142.50-180 and 72.50-110 µg/mL, respectively.

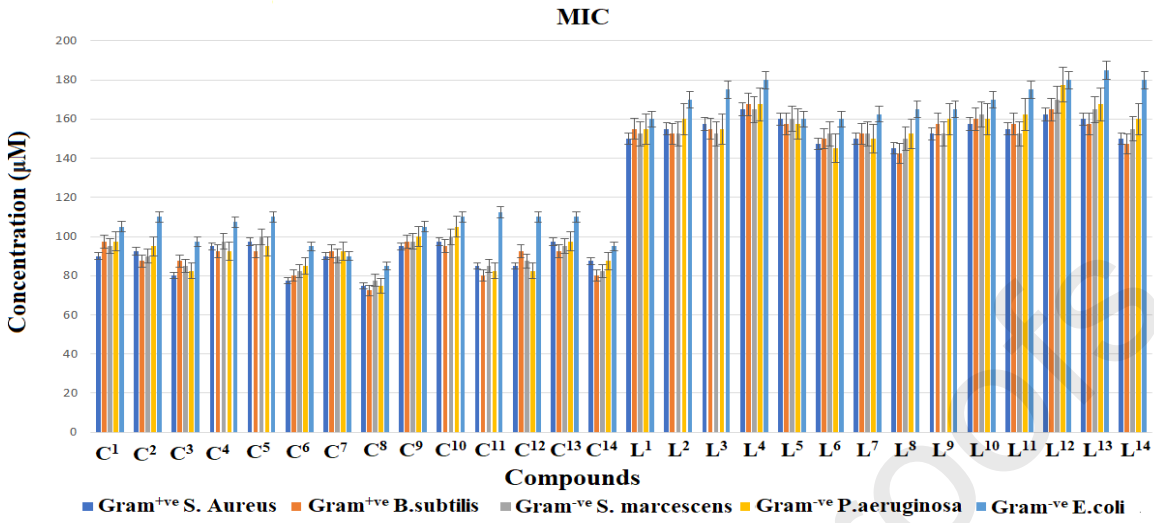

Fig. 5. MIC values of synthesized compounds in **µM**.

3.1.3. Cytotoxicity

Compounds have been stained over *S.Pombe* DNA's cell culture to evaluate their cytotoxic count. With a relative increase in the concentration of DMSO solubilized compounds, relative percentage cell viability increase. Cell death has been observed under a digital microscope. It is concluded that ligands L^1-L^8 dominate in percentage cell viability compared to ligands L^9-L^{14}, the reason is due to the presence of electron pushing functionality on phenyl ring which has less effect in resisting the development of cell growth cycle. Further, their respective Os(IV) complexes also play analogues behavior in potency unlike ligands but they further proved to have more percentage cell viability compared to ligands L^1-L^{14}. Complexes C^1-C^8 show better cytotoxic effect than complexes C^9-C^{14} because of having different classes of ligands. Supplementary material 13 shows the relative percentage cell viability of Os(IV) complexes and their respective ligands. The successive order of percentage cell viability is C^1-C^8 > C^9- C^{14}> L^1-L^8> L^9-L^{14}. Cytotoxicity of Os(IV) complexes have been better than iridium(III) and palladium(II) complexes [40, 41].

Further, cytotoxicity has been evaluated using brine shrimp lethality assay. With the help of the plot, LC_{50} values have been calculated. LC_{50} of ligands L^1-L^{14} fall in the range of 4.00-11.74 µg/mL whereas, osmium(IV) complexes show LC_{50} in the range of 7.92-19.91 µg/mL. The bar graph in figure 6 shows relative LC_{50} of all the synthesized compounds. The reason behind the dominance of Os(IV) complexes is resistance for fertility of brine shrimps, thereby controlling the

pathogenic population by delocalizing the cell growth cycle with the help of nature of groups around the molecule. In ligands, such impactful groups absentia does not play a vital role in resisting growth but heterocyclic π character rich environment and substituents have an optimum effect on resisting brine shrimp growth. Complex C^4 has good cytotoxicity since it possesses nitro functionality at the meta position. Further, complex C^5 has fluorine in the ring which shows comparable but less cytotoxicity compare to complex C^4. Comparing C^1 and C^4, it is observed that both compounds possess chlorine in rings. But one with chlorine at ortho position dominates in cytotoxicity. On widely comparing compounds C^1-C^8 and C^9-C^{14}, former ones have better cytotoxicity effect since C^9-C^{10} has electron releasing functionality which relatively reduces effect.

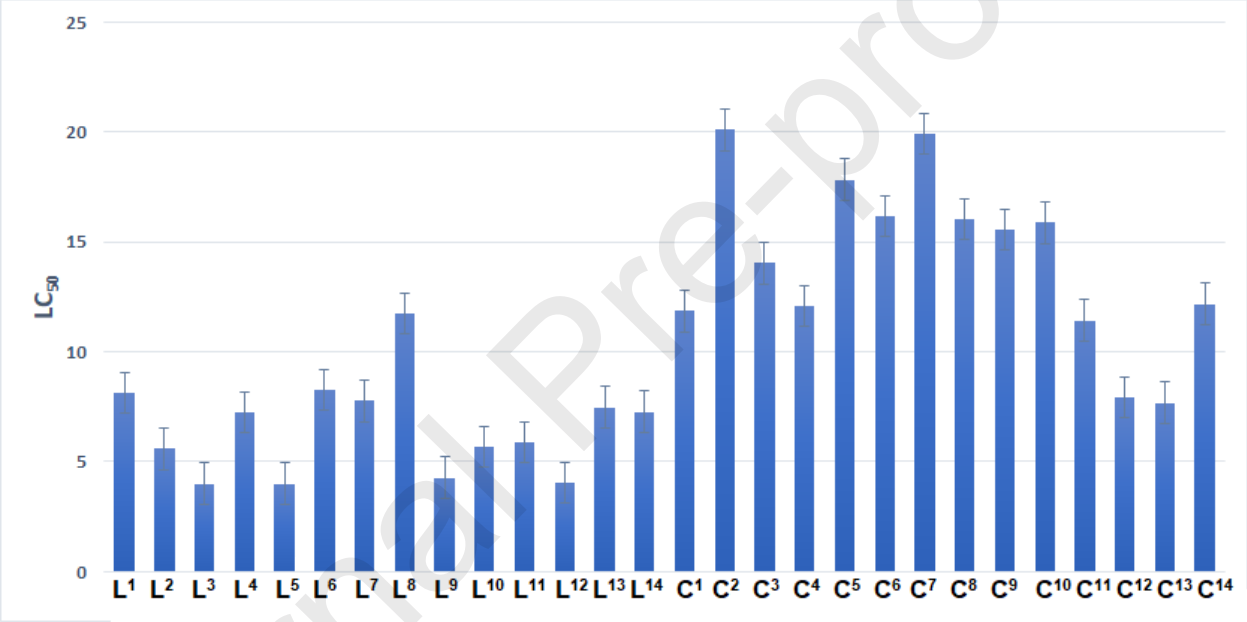

Fig. 6. LC_{50} of ligands and Os(IV) complexes.

IC_{50} values of synthesized compounds have been calculated using HCT-116 lung cancer cell line. IC_{50} values of compounds C^1-C^{14} fall at about 46-1000 µg/mL given in plots mentioned in supplementary material 14. Amongst the complexes C^1-C^8, complex C^4 is the most effective compound. Whereas, amongst the complexes C^9-C^{14} having ligands with 4-hydroxy benzhydrazide, complex C^{13} shows most effective compound, which are dominating in showing antiproliferative activity compared to some of the reported platinum(II) complexes [42]. The reason is the presence of electronegative chlorine atom in respective compounds which dominant in showing cytotoxicity compare to other isostructural compounds with different substituents.

4. Conclusion

In this work, we conclude that compounds show intercalation mode of DNA binding with HS-DNA as observed in absorption titration and docking measurements. The binding constants of complexes fall at about 1.8-7.6×10^4 M^{-1}. Oxadiazole based Os(IV) complexes show better binding compare to reported copper(II) complexes. Whereas compounds C7, C9, and C10 dominate compare to reported platinum ion-based complexes in binding revealed by fluorescence quenching study. LC_{50} values of ligands L^1-L^{14} fall in the range of 4.00-11.74 μg/mL whereas, osmium(IV) complexes show LC_{50} values in the range of 7.92-19.91 μg/mL. The minimum inhibitory concentration of Os(IV) dominates over their respective ligands. Ligands and Os(IV) complexes show MIC in range of 142.50-180 and 72.50-110 μM, respectively. Relative tendency of complexes to show effective smearing is in order of C^3>C^5>C^4>C^1>C^6>C^8>C^2>C^7>C^{13}>C^9>C^{11}>C^{12}>C^{10}>C^{14}. The successive order of percentage cell viability is C^1-C^8 > C^9- C^{14}> L^1-L^8> L^9-L^{14}. Cytotoxicity of Os(IV) complexes have been better than iridium(III) complexes. Amongst the complexes C^1-C^8 having co-ligand benzhydrazide, complex C^4 has the most effective IC_{50}. Whereas, amongst the complexes C^9-C^{14} having co-ligand ligands 4-hydroxy benzhydrazide, complex C^{13} shows the most effective IC_{50} value, which are dominating in showing antiproliferative activity compared to some of reported platinum(II) complexes.

Acknowledgements

The authors are thankful to the Head, Department of Chemistry, Sardar Patel University, Vallabh Vidyanagar, Gujarat, India, for providing the laboratory facilities, U. G. C., New Delhi for providing financial assistance of UGC BSR grant No. C/2015/BSR/Chemistry/1579. Authors are also thankful to UGC-CPEPA and UGC-CAS programmes.

Supporting information: Materials and reagents, Physical measurements, Experimental, ^{1}H-NMR, ^{13}C-NMR, LC-MS, ESI-MS, ICP-OES, Electronic spectrum, IR spectra, CHNS elemental analysis, docking images, biological activities data.

References

[1] S.S. De, M.P. Khambete, M.S. Degani, Oxadiazole scaffolds in anti-tuberculosis drug discovery, Bioorganic & Medicinal Chemistry Letters, 29 (2019) 1999-2007.
[2] N.A. El-Sayed, M.S. Nour, M.A. Salem, R.K. Arafa, New oxadiazoles with selective-COX-2 and EGFR dual inhibitory activity: Design, synthesis, cytotoxicity evaluation and in silico studies, European Journal of Medicinal Chemistry, (2019) 111693.
[3] W. Caneschi, K.B. Enes, C. Carvalho de Mendonça, F. de Souza Fernandes, F.B. Miguel, J. da Silva Martins, M. Le Hyaric, R.R. Pinho, L.M. Duarte, M.A. Leal de Oliveira, H.F. Dos Santos, M.T. Paz Lopes, D. Dittz, H. Silva, M.R. Costa Couri, Synthesis and anticancer evaluation of new lipophilic 1,2,4 and 1,3,4-oxadiazoles, European Journal of Medicinal Chemistry, 165 (2019) 18-30.
[4] H.-Z. Zhang, Z.-L. Zhao, C.-H. Zhou, Recent advance in oxazole-based medicinal chemistry, European Journal of Medicinal Chemistry, 144 (2017).
[5] J. Zhu, J. Mo, H.-z. Lin, Y. Chen, H.-p. Sun, The recent progress of isoxazole in medicinal chemistry, Bioorganic & Medicinal Chemistry, 26 (2018) 3065-3075.
[6] A. Sysak, B. Obmińska-Mrukowicz, Isoxazole ring as a useful scaffold in a search for new therapeutic agents, European Journal of Medicinal Chemistry, 137 (2017) 292-309.
[7] K. Smith, M. Germain, Leflunomide: An Immune Modulating Drug That May Have a Role in Controlling Secondary Infections With Review of Its Mechanisms of Action, Journal of drugs in dermatology : JDD, 14 (2015) 230-234.
[8] A.T.M. Fiori, D.H. Nakahata, A. Cuin, W.R. Lustri, P.P. Corbi, Synthesis, crystallographic studies, high resolution mass spectrometric analyses and antibacterial assays of silver(I) complexes with sulfisoxazole and sulfadimethoxine, Polyhedron, 121 (2017) 172-179.
[9] R. Mesnage, M. Biserni, E. Wozniak, T. Xenakis, C.A. Mein, M.N. Antoniou, Comparison of transcriptome responses to glyphosate, isoxaflutole, quizalofop-p-ethyl and mesotrione in the HepaRG cell line, Toxicology Reports, 5 (2018) 819-826.
[10] X.-p. Ma, J.-s. Chen, X.-h. Du, A Continuous Flow Process for the Synthesis of Hymexazol, Organic Process Research & Development, 23 (2019) 1152-1158.
[11] R. Alikhani, N. Razzaghi-Asl, A. Ramazani, Z. Hosseinzadeh, Insights into the structural/conformational requirements of cytotoxic oxadiazoles as potential chemotherapeutic target binding agents, Journal of Molecular Structure, 1164 (2018) 9-22.
[12] H.-Z. Zhang, Z.-L. Zhao, C.-H. Zhou, Recent advance in oxazole-based medicinal chemistry, European Journal of Medicinal Chemistry, 144 (2018) 444-492.
[13] B. Mochona, X. Qi, S. Euynni, D. Sikazwi, N. Mateeva, K.F. Soliman, Design and evaluation of novel oxadiazole derivatives as potential prostate cancer agents, Bioorganic & Medicinal Chemistry Letters, 26 (2016) 2847-2851.
[14] L.H. Al-Wahaibi, N. Santhosh Kumar, A.A. El-Emam, N.S. Venkataramanan, H.A. Ghabbour, A.-M.S. Al-Tamimi, J. Percino, S. Thamotharan, Investigation of potential anti-malarial lead candidate 2-(4-fluorobenzylthio)-5-(5-bromothiophen-2-yl)-1,3,4-oxadiazole: Insights from crystal structure, DFT, QTAIM and hybrid QM/MM binding energy analysis, Journal of Molecular Structure, 1175 (2019) 230-240.
[15] N. Özbek, S. Alyar, B.K. Memmi, A.B. Gündüzalp, Z. Bahçeci, H. Alyar, Synthesis, characterization, computational studies, antimicrobial activities and carbonic anhydrase inhibitor effects of 2-hydroxy acetophenone-N-methyl p-toluenesulfonylhydrazone and its Co(II), Pd(II), Pt(II) complexes, Journal of Molecular Structure, 1127 (2017) 437-448.
[16] T. Turk, M. Alkhatib, G. Abbas, M.H.D.K. Jawish, O.M. Hammamieh Alshar, H. Abou Alchamat, A. Essali, Risperidone (oral forms) for people with schizophrenia, The Cochrane Database of Systematic Reviews, 2017 (2017) CD012822.

[17] Salahuddin, A. Mazumder, M.S. Yar, R. Mazumder, G.S. Chakraborthy, M.J. Ahsan, M.U. Rahman, Updates on synthesis and biological activities of 1,3,4-oxadiazole: A review, Synthetic Communications, 47 (2017) 1805-1847.
[18] R.M. Shingare, Y.S. Patil, J.N. Sangshetti, R.B. Patil, D.P. Rajani, B.R. Madje, Synthesis, biological evaluation and docking study of some novel isoxazole clubbed 1,3,4-oxadiazoles derivatives, Medicinal Chemistry Research, 27 (2018) 1283-1291.
[19] M.F. Hassan, A. Rauf, Synthesis and multi-spectroscopic DNA binding study of 1,3,4-oxadiazole and 1,3,4-thiadiazole derivatives of fatty acid, Spectrochimica Acta Part A: Molecular and Biomolecular Spectroscopy, 153 (2016) 510-516.
[20] G. Salassa, A. Terenzi, Metal Complexes of Oxadiazole Ligands: An Overview, International Journal of Molecular Sciences, 20 (2019).
[21] C. Tresse, R. Radigue, R. Gomes Von Borowski, M. Thepaut, H. Hanh Le, F. Demay, S. Georgeault, A. Dhalluin, A. Trautwetter, G. Ermel, C. Blanco, P. van de Weghe, M. Jean, J.-C. Giard, R. Gillet, Synthesis and evaluation of 1,3,4-oxadiazole derivatives for development as broad-spectrum antibiotics, Bioorganic & Medicinal Chemistry, 27 (2019) 115097.
[22] M.N. Ahmed, K.A. Yasin, S. Hameed, K. Ayub, I.-u. Haq, M.N. Tahir, T. Mahmood, Synthesis, structural studies and biological activities of three new 2-(pentadecylthio)-5-aryl-1,3,4-oxadiazoles, Journal of Molecular Structure, 1129 (2017) 50-59.
[23] G. Prakash, R. Ramachandran, M. Nirmala, P. Viswanathamurthi, J. Sanmartin, Ruthenium(II) bis(hydrazone) complexes derived from 1,3,4-oxadiazoles: Synthesis, crystal structure and catalytic application in N-alkylation reactions, Inorganica Chimica Acta, 427 (2015) 203-210.
[24] R.B. Singh, N. Das, G.K. Singh, S.K. Singh, K. Zaman, Synthesis and pharmacological evaluation of 3-[5-(aryl-[1,3,4]oxadiazole-2-yl]-piperidine derivatives as anticonvulsant and antidepressant agents, Arabian Journal of Chemistry, 13 (2020) 5299-5311.
[25] M. Akhtar, S.U. Khan, D.-X. Zhu, G.-G. Shan, Z.-M. Su, Synthesis, characterization, photo-and-electrochemical properties of cationic iridium(III) complexes by using 1,3,4-oxadiazole cyclometallating ligand, Inorganic Chemistry Communications, 118 (2020) 107980.
[26] I.E. Mikhailov, G.A. Dushenko, M.E. Gurskii, N.I. Vikrischuk, L.D. Popov, Y.V. Revinskii, K.A. Lyssenko, V.I. Minkin, Synthesis, structure, spectral and luminescence properties of the tetracoordinated diphenylboron and zinc complexes with 1,3,4-oxadiazole and 1,2,4-triazole ligands, Polyhedron, 166 (2019) 73-82.
[27] G. Munikumari, R. Konakanchi, V.B. Nishtala, G. Ramesh, L.R. Kotha, K.B. Chandrasekhar, C. Ramachandraiah, Palladium(II) complexes of 5-substituted isatin thiosemicarbazones: Synthesis, spectroscopic characterization, biological evaluation and in silico docking studies, Synthetic Communications, 49 (2019) 146-158.
[28] S.M. Meier-Menches, C. Gerner, W. Berger, C.G. Hartinger, B.K. Keppler, Structure–activity relationships for ruthenium and osmium anticancer agents – towards clinical development, Chemical Society Reviews, 47 (2018) 909-928.
[29] C. Sanchez-Cano, I. Romero-Canelón, K. Geraki, P.J. Sadler, Microfocus x-ray fluorescence mapping of tumour penetration by an organo-osmium anticancer complex, Journal of Inorganic Biochemistry, 185 (2018) 26-29.
[30] B.H. Pursuwani, B.S. Bhatt, F.U. Vaidya, C. Pathak, M.N. Patel, Tetrazolo[1,5-a]quinoline moiety-based Os(IV) complexes: DNA binding/cleavage, bacteriostatic and photocytotoxicity assay, Journal of Biomolecular Structure and Dynamics, (2020) 1-10.
[31] K. Li, Supramolecular Ruthenium(II) and Osmium(II) Complexes: Synthesis, Characterization, DNA Binding and DNA Photocleavage, in, University of Dayton, 2017.

[32] T. Nabiyeva, C. Marschner, B. Blom, Synthesis, structure and anti-cancer activity of osmium complexes bearing π-bound arene substituents and phosphane Co-Ligands: A review, European Journal of Medicinal Chemistry, (2020) 112483.
[33] Y. Fu, A. Habtemariam, A.M. Pizarro, S.H. van Rijt, D.J. Healey, P.A. Cooper, S.D. Shnyder, G.J. Clarkson, P.J. Sadler, Organometallic Osmium Arene Complexes with Potent Cancer Cell Cytotoxicity, Journal of Medicinal Chemistry, 53 (2010) 8192-8196.
[34] S.D. Shnyder, Y. Fu, A. Habtemariam, S.H. van Rijt, P.A. Cooper, P.M. Loadman, P.J. Sadler, Anti-colorectal cancer activity of an organometallic osmium arene azopyridine complex, MedChemComm, 2 (2011) 666-668.
[35] P.A. Lay, A.M. Sargeson, Tris(1,2-ethanediamine) complexes of osmium(IV), osmium(III) and osmium(II): oxidative dehydrogenation reactions, Inorganica Chimica Acta, 198-200 (1992) 449-460.
[36] K. Maruyama, Y. Mishima, K. Minagawa, J. Motonaka, Electrochemical and DNA-binding properties of dipyridophenazine complexes of osmium(II), 2001.
[37] G.E. Büchel, I.N. Stepanenko, M. Hejl, M.A. Jakupec, B.K. Keppler, P. Heffeter, W. Berger, V.B. Arion, Osmium(IV) complexes with 1H- and 2H-indazoles: Tautomer identity versus spectroscopic properties and antiproliferative activity, Journal of Inorganic Biochemistry, 113 (2012) 47-54.
[38] P. Zhang, H. Huang, Future potential of osmium complexes as anticancer drug candidates, photosensitizers and organelle-targeted probes, Dalton Transactions, 47 (2018) 14841-14854.
[39] J.V. Mehta, S.B. Gajera, D.D. Patel, M.N. Patel, Synthesis, spectral investigation and development of tetrahedral copper(II) complexes as artificial metallonucleases and antimalarial agents, Applied Organometallic Chemistry, 29 (2015) 357-367.
[40] K.P. Thakor, M.V. Lunagariya, B.S. Bhatt, M.N. Patel, Fluorescence and absorption studies of DNA–Pd(II) complex interaction: Synthesis, spectroanalytical investigations and biological activities, Luminescence, 34 (2019) 113-124.
[41] P.A. Vekariya, P.S. Karia, B.S. Bhatt, M.N.J.A.b. Patel, biotechnology, Half sandwich rhodium (III) and iridium (III) complexes as cytotoxic and metallonuclease agents, 187 (2019) 556-569.
[42] J. Zhao, S. Gou, Y. Sun, L. Fang, Z. Wang, Antitumor Platinum(II) Complexes Containing Platinum-Based Moieties of Present Platinum Drugs and Furoxan Groups as Nitric Oxide Donors: Synthesis, DNA Interaction, and Cytotoxicity, Inorganic Chemistry, 51 (2012) 10317-10324.

Highlights

- Os(IV) compounds show good binding strength and intercalation mode of binding with HS-DNA.
- Os(IV) compounds show effective impact on displacing intercalator ethidium bromine in fluorescence quenching study..
- Os(IV) compounds show good cytotoxicity over different sets of assays viz. percentage cell viability on *S. Pombe* cell and BSLA.
- Os(IV) compounds show good antiproliferative activity against human cancer cell line HCT-116.